AIMS Mathematics, 11(3): 6569–6591.
DOI: 10.3934/math.2026272
Received: 28 January 2026
Revised: 02 March 2026
Accepted: 06 March 2026
Published: 13 March 2026

https://www.aimspress.com/journal/Math

Research article

Hopf bifurcation analysis of a modified Brusselator model with sub-interval distributed delay

Shouzong Liu[1,2,*], **Tingting Lu**[1], **Jianing Qin**[1] **and Yaxin Niu**[1]

[1] School of Mathematics and Statistics, Xinyang Normal University, Xinyang 464000, China

[2] Henan Provincial Center for Applied Mathematics, Xinyang Normal University, Xinyang 464000, China

* **Correspondence:** Email: liushouzong@163.com.

Abstract: In this paper, a modified Brusselator model incorporating a moderated autocatalytic term and a sub-interval distributed delay is investigated. The existence and uniqueness of a positive equilibrium are first established, together with explicit conditions for its local asymptotic stability. By deriving and analyzing the associated characteristic equation, two distinct Hopf bifurcation mechanisms are rigorously identified: one induced by variations in the delay center τ and the other triggered by changes in the delay distribution width ε. Sufficient conditions for the existence of two Hopf bifurcation branches in the (τ, ε)-parameter plane are obtained, and the corresponding transversality conditions are verified. Finally, numerical simulations are carried out to validate the theoretical results. The results reveal a clear destabilizing role of the delay center and a stabilizing, smoothing effect of the delay width, which highlights the important role of distributed delays in shaping the dynamical behavior of autocatalytic reaction systems.

Keywords: Brusselator model; sub-interval distributed delay; Hopf bifurcation; stability
Mathematics Subject Classification: 34K18, 34K20, 37G15

1. Introduction

Nonlinear reaction systems with autocatalytic feedback have long served as fundamental models for understanding oscillatory phenomena in chemical and biological processes [1–3]. Among these, the Brusselator system is widely recognized as a prototypical example that captures self-sustained oscillations arising from nonlinear interactions between reactants [4, 5]. Owing to its simple structure and rich dynamical behavior, the Brusselator has been extensively studied as a benchmark model in nonlinear dynamics [6, 7], bifurcation theory [8–10], and pattern formation [11–13].

The classical Brusselator model is given by [14]

$$\begin{cases} \dfrac{dX}{dt} = a - (b+1)X + X^2Y, \\ \dfrac{dY}{dt} = bX - X^2Y, \end{cases} \tag{1.1}$$

where $X(t)$ and $Y(t)$ denote the concentrations of two interacting reactants, and $a, b > 0$ are constant reaction parameters. The quadratic term X^2Y represents an autocatalytic reaction mechanism, which plays a central role in destabilizing the equilibrium and generating oscillatory dynamics.

Despite its success as a conceptual model, the classical Brusselator model relies on two simplifying assumptions that may limit its applicability to realistic reaction networks. First, the quadratic autocatalytic term implies that the reaction rate increases indefinitely with the activator concentration X. However, in practical chemical and biological systems, autocatalytic efficiency is often limited by finite reaction sites, intermediate resource availability, or transport effects [15, 16], which weakens feedback strength at high concentrations. Second, the classical model assumes reaction rates depend instantaneously on the current system state, thus ignoring time delays from multistep reaction pathways, signal transduction processes, or regulatory feedback mechanisms [17, 18].

To address the first limitation, various modified autocatalytic terms have been proposed in the literature to reduce the effective reaction order while preserving the essential nonlinear structure of the Brusselator model [19]. In this work, we use a moderated autocatalytic term $\frac{cX^2Y}{1+X}$, which introduces a subquadratic growth mechanism. This formulation does not set a strict upper limit on the reaction rate. Instead, it shows reduced autocatalytic efficiency as X increases, thus providing a more realistic description of autocatalytic feedback in high-concentration systems.

In recent years, discrete-delay models have been widely studied in ecological and epidemiological contexts, where delays represent maturation periods, intracellular infection processes, or immune response times [20–22]. These studies demonstrate that time lags may destabilize equilibria and induce Hopf bifurcations, leading to complex oscillatory dynamics.

Motivated by these developments, time-delay mechanisms have also been incorporated into classical chemical reaction models such as the Brusselator. Numerous previous works have extended the Brusselator framework by introducing discrete delays, where the reaction rate depends on the system state at a single past instant [23–25]. These discrete-delay Brusselator models further reveal the destabilizing role of delayed feedback and the rich bifurcation structures arising from delay interactions.

Nevertheless, the discrete delay assumption implicitly presumes that the system responds to an exact historical state, an idealization that may not hold in many practical applications [26]. In contrast, distributed delays incorporate accumulated or averaged memory effects over a finite time interval. Such formulations have been investigated, for example, in neural oscillation models and cortex-basal ganglia networks with heterogeneous delay distributions [27,28], where distributed delays significantly influence Hopf bifurcation mechanisms.

Motivated by this observation, we introduce a sub-interval distributed delay into the Brusselator framework. Such a delay formulation captures finite-memory effects by averaging the past state over a prescribed time window, thereby providing a natural generalization of discrete delays. Importantly, the sub-interval distributed delay is characterized by two independent parameters: the center of the delay distribution and its width. This additional degree of freedom allows for a more flexible

representation of temporal dispersion and leads to dynamical behaviors that cannot be captured by discrete delays [29, 30].

Combining the above two modeling considerations, we propose the following modified Brusselator system

$$\begin{cases} \dfrac{dX}{dt} = a - (b+1)L(X_t) + \dfrac{cX^2Y}{1+X}, \\ \dfrac{dY}{dt} = bX - \dfrac{cX^2Y}{1+X}, \end{cases} \tag{1.2}$$

subject to the initial conditions

$$X(t) = u(t) > 0, \quad Y(t) = v(t) > 0, \quad t \in [-\tau - \varepsilon, 0]. \tag{1.3}$$

Here $a, b, c > 0$ are constant parameters, and the delayed feedback is described by

$$L(X_t) = \frac{1}{2\varepsilon} \int_{-\tau-\varepsilon}^{-\tau+\varepsilon} X(t+\theta)\, d\theta, \tag{1.4}$$

where $\tau > 0$ denotes the center of the delay distribution and $\varepsilon \in [0, \tau)$ represents its half-width. This formulation generalizes the discrete-delay case, which is recovered when $\varepsilon = 0$ since

$$\lim_{\varepsilon \to 0} L(X_t) = \lim_{\varepsilon \to 0} \frac{X(t-\tau+\varepsilon) + X(t-\tau-\varepsilon)}{2} = X(t-\tau).$$

Thus, it provides a natural representation of finite-memory effects arising from temporal dispersion in reaction processes. Unlike classical discrete delays, the sub-interval distributed delay introduces two independent parameters (τ and ε) that characterize both the location and the width of the past influence, leading to a richer dynamical structure.

The primary objective of this paper is to investigate how the combined effects of moderated autocatalysis and sub-interval distributed delay influence the dynamical behavior of the Brusselator system (1.2). In particular, we focus on the stability of the positive equilibrium and the emergence of oscillatory solutions through Hopf bifurcation induced by the delay parameters τ and ε. Special attention is paid to the interaction between the location and the width of the delay distribution, which leads to a richer bifurcation structure in the (τ, ε)-parameter plane than that observed in classical discrete delay models.

The remainder of this paper is organized as follows. In Section 2, we analyze the existence and stability of the positive equilibrium and derive the corresponding characteristic equation. In addition, conditions for Hopf bifurcation are obtained, and the effects of the delay parameters on system dynamics are explored. In Section 3, numerical simulations are conducted to validate the theoretical findings. Finally, brief conclusions are given in Section 4.

2. Equilibria and Hopf bifurcation analysis

In this section, we aim to analyze the existence and stability of the positive equilibrium points of the modified Brusselator system (1.2) and investigate its Hopf bifurcation behavior induced by the delay parameters τ and ε.

2.1. Positive equilibrium and its local stability

The equilibria of system (1.2) correspond to the nonnegative solutions of the following algebraic system:

$$\begin{cases} a-(b+1)X^*+\dfrac{c(X^*)^2}{1+X^*}Y^*=0, \\ bX^*-\dfrac{c(X^*)^2}{1+X^*}Y^*=0. \end{cases}$$

A direct calculation shows that this system admits a unique positive equilibrium:

$$E^*=(X^*,Y^*)=\left(a,\ \frac{(1+a)b}{ca}\right).$$

We now proceed to investigate the stability of E^*.

Theorem 2.1. *Assume that the model parameters satisfy*

$$\frac{ca^2}{1+a}>\max\left\{0,\ \frac{b}{1+a}-1\right\}, \tag{2.1}$$

and that the delay parameter τ satisfies

$$\tau<\frac{ca^2-b}{ca^2(1+b)}. \tag{2.2}$$

Then, the positive equilibrium

$$E^*=\left(a,\ \frac{(1+a)b}{ca}\right)$$

of system (1.2) *is locally asymptotically stable.*

Proof. To investigate the local stability of the equilibrium E^*, we introduce the perturbation variables

$$x(t)=X(t)-X^*,\qquad y(t)=Y(t)-Y^*,$$

which represent deviations from the equilibrium. Substituting these into system (1.2) and expanding around E^* yields the linearized system:

$$\begin{cases} \dfrac{dx}{dt}=-(b+1)L(x_t)+\dfrac{b(2+a)}{1+a}\,x(t)+\dfrac{ca^2}{1+a}\,y(t), \\ \dfrac{dy}{dt}=-\dfrac{b}{1+a}\,x(t)-\dfrac{ca^2}{1+a}\,y(t). \end{cases} \tag{2.3}$$

Thus, the stability of E^* is equivalent to the stability of the zero solution of system (2.3).

To derive the characteristic equation, we seek exponential solutions of the form $x(t)=x_0e^{\lambda t}$, $y(t)=y_0e^{\lambda t}$, where $\lambda\in\mathbb{C}$ and x_0,y_0 are constants. Substituting into (2.3) yields

$$\lambda x_0e^{\lambda t}=-(b+1)L(x_t)+\frac{b(2+a)}{1+a}x_0e^{\lambda t}+\frac{ca^2}{1+a}y_0e^{\lambda t},$$

$$\lambda y_0 e^{\lambda t} = -\frac{b}{1+a} x_0 e^{\lambda t} - \frac{ca^2}{1+a} y_0 e^{\lambda t}.$$

Noting that $L(x_t) = x_0 e^{\lambda t} L(e^{\lambda t})$ with

$$L(e^{\lambda t}) = \frac{1}{2\epsilon} \int_{-\tau-\epsilon}^{-\tau+\epsilon} e^{\lambda\theta} d\theta = \frac{1}{2\epsilon\lambda} \left(e^{-(\tau-\epsilon)\lambda} - e^{-(\tau+\epsilon)\lambda} \right), \tag{2.4}$$

we cancel the common factor $e^{\lambda t}$ and obtain

$$\left(\lambda + (b+1)L(e^{\lambda t}) - \frac{b(2+a)}{1+a} \right) x_0 - \frac{ca^2}{1+a} y_0 = 0,$$

$$\frac{b}{1+a} x_0 + \left(\lambda + \frac{ca^2}{1+a} \right) y_0 = 0.$$

For nontrivial solutions, the determinant of the coefficient matrix must vanish:

$$\det \begin{pmatrix} \lambda + (b+1)L(e^{\lambda t}) - \frac{b(2+a)}{1+a} & -\frac{ca^2}{1+a} \\ \frac{b}{1+a} & \lambda + \frac{ca^2}{1+a} \end{pmatrix} = 0.$$

Expanding the determinant gives

$$\left(\lambda + (b+1)L(e^{\lambda t}) - \frac{b(2+a)}{1+a} \right) \left(\lambda + \frac{ca^2}{1+a} \right) + \frac{ca^2 b}{(1+a)^2} = 0.$$

After simplification, we obtain the characteristic equation

$$F(\lambda) = \lambda^2 + \frac{1}{1+a}(ca^2 - ab - 2b)\lambda + (b+1)\left(\lambda + \frac{ca^2}{1+a}\right)L(e^{\lambda\tau}) - \frac{ca^2 b}{1+a} = 0. \tag{2.5}$$

We first examine the case without delay, i.e., $\tau = \varepsilon = 0$. In this situation $L(e^{\lambda\tau}) = 1$, and (2.5) reduces to

$$\lambda^2 + \left(1 + \frac{ca^2}{1+a} - \frac{b}{1+a}\right)\lambda + \frac{ca^2}{1+a} = 0.$$

Under condition (2.1), all coefficients of this quadratic polynomial are positive. By the Routh–Hurwitz criterion, the zero solution of (2.3) is locally asymptotically stable, and consequently E^* is locally asymptotically stable when $\tau = \varepsilon = 0$.

We now consider the distributed delay case with $\tau > \varepsilon > 0$. Substituting the explicit form of the delay operator (2.4) into (2.5) gives

$$\begin{aligned} F(\lambda) = \lambda^2 &+ \frac{1}{1+a}(ca^2 - ab - 2b)\lambda - \frac{ca^2 b}{1+a} \\ &+ \frac{b+1}{2\varepsilon\lambda}\left(\lambda + \frac{ca^2}{1+a}\right)\left(e^{(-\tau+\varepsilon)\lambda} - e^{-(\tau+\varepsilon)\lambda}\right) = 0. \end{aligned} \tag{2.6}$$

Suppose that stability is lost at some $\tau > 0$. Then there exists $\omega > 0$ such that $\lambda = i\omega$ satisfies the characteristic equation (2.6). Substituting $\lambda = i\omega$ and separating real and imaginary parts yields

$$-\omega^2 - \frac{ca^2 b}{1+a} + \frac{ca^2(b+1)}{\varepsilon(1+a)\omega} \sin(\omega\varepsilon)\cos(\omega\tau) + \frac{b+1}{\varepsilon} \sin(\omega\tau)\sin(\omega\varepsilon) = 0, \tag{2.7}$$

$$\frac{ca^2 - b(a+2)}{1+a}\omega + \frac{b+1}{\varepsilon}\sin(\omega\varepsilon)\cos(\omega\tau) - \frac{ca^2(b+1)}{\varepsilon(1+a)\omega}\sin(\omega\tau)\sin(\omega\varepsilon) = 0. \tag{2.8}$$

Algebraic manipulation of (2.7) and (2.8) leads to

$$\frac{ca^2(ca^2-b)}{(1+a)^2} + \omega^2 = \frac{b+1}{\varepsilon}\left[1 + \frac{c^2a^4}{(1+a)^2\omega^2}\right]\sin(\omega\tau)\sin(\omega\varepsilon).$$

By direct calculation, we get

$$\frac{1}{(b+1)\left[\dfrac{c^2a^4}{(1+a)^2} + \omega^2\right]}\left[\frac{ca^2(ca^2-b)}{(1+a)^2} + \omega^2\right] = \tau\,\frac{\sin(\omega\tau)}{\omega\tau}\,\frac{\sin(\omega\varepsilon)}{\omega\varepsilon} \le \tau. \tag{2.9}$$

Denote the left-hand side of (2.9) by $H(\omega)$. It can be verified that $H(\omega)$ is strictly increasing with respect to $\omega > 0$. Evaluate the limits:

$$H(0^+) = \frac{ca^2(ca^2-b)}{(1+a)^2}\cdot\frac{(1+a)^2}{(b+1)c^2a^4} = \frac{ca^2-b}{(b+1)ca^2},$$

$$\lim_{\omega\to+\infty} H(\omega) = \frac{1}{b+1}.$$

Thus, $H(\omega)$ ranges over the interval

$$\left(\frac{ca^2-b}{(b+1)ca^2},\ \frac{1}{b+1}\right) \quad \text{for } \omega > 0.$$

Hence, if condition (2.2) holds, Eq (2.9) admits no solution for any $\omega > 0$, which means the characteristic equation has no purely imaginary roots.

Combining this observation with the stability established for $\tau = \varepsilon = 0$ and the continuous dependence of eigenvalues on the delay parameters, we conclude that E^* remains locally asymptotically stable whenever conditions (2.1) and (2.2) are satisfied. The proof is complete. □

2.2. Analysis of Hopf bifurcation

In the following, we focus on the Hopf bifurcation of the modified Brusselator system with respect to the delay parameters: the time delay center τ and the delay distribution width ε. Specifically, we derive two distinct bifurcation conditions corresponding to each parameter, which characterize the transition between stable equilibrium to oscillatory solutions. This analysis is crucial for elucidating the system's dynamical behavior under varying time delay structures.

2.2.1. Hopf bifurcation with respect to the delay center τ

We first explore the bifurcation induced by τ, and examinate how it affects the system's stability and oscillatory dynamics.

Let

$$\Delta_1 = \cos(\omega\tau)\sin(\omega\varepsilon), \qquad \Delta_2 = \sin(\omega\tau)\sin(\omega\varepsilon).$$

Then, the real and imaginary part equations (2.7) and (2.8) can be rewritten equivalently as

$$-\omega^2 - \frac{ca^2b}{1+a} + \frac{ca^2(b+1)}{\varepsilon(1+a)\omega}\Delta_1 + \frac{b+1}{\varepsilon}\Delta_2 = 0, \tag{2.10}$$

$$\frac{ca^2 - b(a+2)}{1+a}\omega + \frac{b+1}{\varepsilon}\Delta_1 - \frac{ca^2(b+1)}{\varepsilon(1+a)\omega}\Delta_2 = 0. \tag{2.11}$$

Solving (2.10) and (2.11) for Δ_1 and Δ_2 yields

$$\Delta_2 = \frac{\varepsilon\omega^2[ca^2(ca^2-b) + (1+a)^2\omega^2]}{(b+1)[c^2a^4 + (1+a)^2\omega^2]}, \tag{2.12}$$

$$\Delta_1 = \frac{\varepsilon\omega b[c^2a^4 + (1+a)(2+a)\omega^2]}{(b+1)[c^2a^4 + (1+a)^2\omega^2]}. \tag{2.13}$$

These expressions satisfy the relations

$$\Delta_1^2 + \Delta_2^2 = \frac{\varepsilon^2\omega^2}{(b+1)^2[c^2a^4 + (1+a)^2\omega^2]}\,\kappa, \tag{2.14}$$

$$\frac{\Delta_1}{\Delta_2} = \frac{b[c^2a^4 + (1+a)(2+a)\omega^2]}{\omega[ca^2(ca^2-b) + (1+a)^2\omega^2]} = \cot(\omega\tau), \tag{2.15}$$

where

$$\kappa = (1+a)^2\omega^4 + [b^2(1+a)(3+a) + (a^2c-b)^2]\omega^2 + a^4b^2c^2.$$

From (2.15), we obtain an expression for τ in terms of ω:

$$\tau = \frac{1}{\omega}\operatorname{arccot}\left(\frac{b[c^2a^4 + (1+a)(2+a)\omega^2]}{\omega[ca^2(ca^2-b) + (1+a)^2\omega^2]}\right). \tag{2.16}$$

Since $\Delta_1^2 + \Delta_2^2 = \sin^2(\omega\varepsilon)$, combining (2.14) and (2.16) leads to the following system linking ω and τ:

$$\begin{cases} \kappa = \dfrac{(b+1)^2[c^2a^4 + (1+a)^2\omega^2]}{\varepsilon^2\omega^2}\sin^2(\omega\varepsilon), \\ \tau = \dfrac{1}{\omega}\operatorname{arccot}\left(\dfrac{b[c^2a^4 + (1+a)^2\omega^2]}{\omega[ca^2(ca^2-b) + (1+a)^2\omega^2]}\right). \end{cases} \tag{2.17}$$

Define the function

$$\begin{aligned} p(\omega) &= \kappa - \frac{(b+1)^2[c^2a^4 + (1+a)^2\omega^2]}{\varepsilon^2\omega^2}\sin^2(\omega\varepsilon) \\ &= (1+a)^2\omega^4 + [b^2(1+a)(3+a) + (a^2c-b)^2]\omega^2 + a^4b^2c^2 \\ &\quad - \frac{(b+1)^2[c^2a^4 + (1+a)^2\omega^2]}{\varepsilon^2\omega^2}\sin^2(\omega\varepsilon). \end{aligned} \tag{2.18}$$

A direct calculation gives

$$p(0) = a^4c^2[b^2 - (b+1)^2] < 0,$$

and

$$p\left(\frac{\pi}{\varepsilon}\right) = (1+a)^2\left(\frac{\pi}{\varepsilon}\right)^4 + [b^2(1+a)(3+a) + (a^2c-b)^2]\left(\frac{\pi}{\varepsilon}\right)^2 + a^4b^2c^2 > 0.$$

Now, to evaluate $p\left(\frac{\pi}{2\varepsilon}\right)$, we note that $\sin(\pi/2) = 1$, so

$$\begin{aligned} p\left(\frac{\pi}{2\varepsilon}\right) &= (1+a)^2\left(\frac{\pi}{2\varepsilon}\right)^4 + [b^2(1+a)(3+a) + (a^2c-b)^2]\left(\frac{\pi}{2\varepsilon}\right)^2 + a^4b^2c^2 \\ &\quad - \frac{(b+1)^2[c^2a^4 + (1+a)^2\left(\frac{\pi}{2\varepsilon}\right)^2]}{\varepsilon^2\left(\frac{\pi}{2\varepsilon}\right)^2}\sin^2\left(\frac{\pi}{2}\right) \\ &= (1+a)^2\frac{\pi^4}{16\varepsilon^4} + [b^2(1+a)(3+a) + (a^2c-b)^2]\frac{\pi^2}{4\varepsilon^2} + a^4b^2c^2 \\ &\quad - \frac{4(b+1)^2}{\pi^2}c^2a^4 - \frac{(b+1)^2(1+a)^2}{\varepsilon^2}. \end{aligned}$$

Grouping the terms with $(\pi/2\varepsilon)^2$ and $(\pi/2\varepsilon)^4$, we have

$$\begin{aligned} p\left(\frac{\pi}{2\varepsilon}\right) &= (1+a)^2\left(\frac{\pi}{2\varepsilon}\right)^4 + \left[b^2(1+a)(3+a) + (a^2c-b)^2 - \frac{4(b+1)^2(1+a)^2}{\pi^2}\right]\left(\frac{\pi}{2\varepsilon}\right)^2 \\ &\quad + a^4c^2\left(b^2 - \frac{4(b+1)^2}{\pi^2}\right). \end{aligned}$$

Suppose that

$$b < \frac{2}{\pi-2} \quad \text{and} \quad \varepsilon > \varepsilon_0, \tag{2.19}$$

where

$$\varepsilon_0 = \pi(1+a)\left\{2\left[-b^2(1+a)(3+a) - (a^2c-b)^2 + \frac{4(b+1)^2(1+a)^2}{\pi^2} + x_0\right]\right\}^{-\frac{1}{2}},$$

$$x_0 = \sqrt{\left(b^2(1+a)(3+a) + (a^2c-b)^2 - \frac{4(b+1)^2(1+a)^2}{\pi^2}\right)^2 - 4(1+a)^2a^4c^2\left(b^2 - \frac{4(b+1)^2}{\pi^2}\right)}.$$

Then $p\left(\frac{\pi}{2\varepsilon}\right) < 0$. Consequently, there exists at least one $\omega^* \in \left(\frac{\pi}{2\varepsilon}, \frac{\pi}{\varepsilon}\right)$ such that $p(\omega^*) = 0$.

Moreover, differentiating $p(\omega)$ yields

$$\begin{aligned} p'(\omega) &= 4(1+a)^2\omega^3 + 2[b^2(1+a)(3+a) + (a^2c-b)^2]\omega \\ &\quad - \frac{(b+1)^2[a^4c^2 + (1+a)^2\omega^2]}{\varepsilon^2\omega^2}\sin(2\omega\varepsilon) + \frac{2a^4(1+b)^2c}{\varepsilon^2\omega^3}\sin^2(\omega\varepsilon). \end{aligned} \tag{2.20}$$

For $\omega \in \left(\frac{\pi}{2\varepsilon}, \frac{\pi}{\varepsilon}\right)$, we have $2\omega\varepsilon \in (\pi, 2\pi)$, and hence $\sin(2\omega\varepsilon) < 0$, which implies $p'(\omega) > 0$. Therefore, $p(\omega)$ is strictly increasing on this interval. We thus obtain the following result.

Lemma 2.1. *If $\varepsilon > \varepsilon_0$ and $b < \frac{2}{\pi-2}$, then the function $p(\omega)$ admits a unique zero:*

$$\omega^* \in \left(\frac{\pi}{2\varepsilon}, \frac{\pi}{\varepsilon}\right).$$

By Lemma 2.1, there exists $\omega^* > 0$ such that $F(i\omega^*) = 0$. This leads to the following Hopf bifurcation result.

Theorem 2.2. *Assume that $\varepsilon > \varepsilon_0$ and $b < \dfrac{2}{\pi - 2}$. Let*

$$\tau^* = \frac{1}{\omega^*}\operatorname{arccot}\left(\frac{b[c^2a^4 + (1+a)(2+a)(\omega^*)^2]}{\omega^*[ca^2(ca^2-b) + (1+a)^2(\omega^*)^2]}\right), \tag{2.21}$$

where ω^* is the unique positive zero of the function $p(\omega)$ in the interval $\left(\frac{\pi}{2\varepsilon}, \frac{\pi}{\varepsilon}\right)$. Then, as the delay parameter τ increases from values less than τ^* to values greater than τ^*, system (1.2) *undergoes a Hopf bifurcation at the equilibrium E^*.*

Proof. To establish the occurrence of a Hopf bifurcation, it suffices to verify the transversality condition

$$\left.\frac{d\,\mathrm{Re}(\lambda)}{d\tau}\right|_{\tau=\tau^*} > 0,$$

which ensures that the real part of the critical eigenvalue crosses the imaginary axis with nonzero speed as τ varies.

Differentiating the characteristic equation (2.5) implicitly with respect to τ yields

$$\left(\frac{d\lambda}{d\tau}\right)^{-1} = \frac{2\varepsilon\left(2\lambda + \frac{ca^2-b(a+2)}{1+a}\right)}{(\lambda + \frac{ca^2}{1+a})(b+1)[e^{(-\tau+\varepsilon)\lambda} - e^{(-\tau-\varepsilon)\lambda}]} - \frac{\frac{ca^2}{1+a}}{\lambda^2(\lambda + \frac{ca^2}{1+a})} - \frac{\tau}{\lambda} + \frac{\varepsilon}{\lambda}\frac{e^{(-\tau+\varepsilon)\lambda} + e^{(-\tau-\varepsilon)\lambda}}{e^{(-\tau+\varepsilon)\lambda} - e^{(-\tau-\varepsilon)\lambda}}.$$

Evaluating this expression at $\tau = \tau^*$ and $\lambda = i\omega^*$, we find

$$\operatorname{sgn}\left\{\left.\frac{d\,\mathrm{Re}(\lambda)}{d\tau}\right|_{\tau=\tau^*}\right\} = \operatorname{sgn}\left\{\mathrm{Re}\left[\left(\frac{d\lambda}{d\tau}\right)^{-1}\Big|_{\tau=\tau^*}\right]\right\}. \tag{2.22}$$

A direct calculation shows that the real part can be expressed as

$$\begin{aligned}
&\mathrm{Re}\left[\left(\frac{d\lambda}{d\tau}\right)^{-1}\Big|_{\tau=\tau^*}\right] \\
&= \mathrm{Re}\Bigg[\frac{2\varepsilon(2i\omega^* + \frac{ca^2-b(a+2)}{1+a})}{(b+1)\left(i\omega^* + \frac{ca^2}{1+a}\right)(e^{(-\tau^*+\varepsilon)i\omega^*} - e^{(-\tau^*-\varepsilon)i\omega^*})} \\
&\quad + \frac{\frac{ca^2}{1+a}}{\omega^{*2}\left(i\omega^* + \frac{ca^2}{1+a}\right)} + \frac{\varepsilon}{i\omega^*}\cdot\frac{\left(e^{(-\tau^*+\varepsilon)i\omega^*} + e^{(-\tau^*-\varepsilon)i\omega^*}\right)}{(e^{(-\tau^*+\varepsilon)i\omega^*} - e^{(-\tau^*-\varepsilon)i\omega^*})}\Bigg] \\
&= \mathrm{Re}\Bigg[\frac{\frac{ca^2}{1+a}(\frac{ca^2}{1+a} - i\omega^*)}{\omega^{*2}(\frac{c^2a^4}{(1+a)^2} + \omega^{*2})} + \frac{\varepsilon}{i\omega^*}\cdot\frac{C_\varepsilon C_\tau - iS_\tau C_\varepsilon}{S_\varepsilon S_\tau + iS_\varepsilon C_\tau} + \frac{\varepsilon\left(2i\omega^* + \frac{ca^2-b(a+2)}{1+a}\right)}{\left(i\omega^* + \frac{ca^2}{1+a}\right)(b+1)\,(S_\varepsilon S_\tau + iS_\varepsilon C_\tau)}\Bigg] \\
&= \mathrm{Re}\Bigg[\frac{\frac{ca^2}{1+a}(\frac{ca^2}{1+a} - i\omega^*)}{\omega^{*2}(\frac{c^2a^4}{(1+a)^2} + \omega^{*2})} - \frac{\varepsilon}{i\omega^*}\cdot\frac{C_\varepsilon}{S_\varepsilon} + \frac{\varepsilon\left(2i\omega^* + \frac{ca^2-b(a+2)}{1+a}\right)\left(\frac{ca^2}{1+a} - i\omega^*\right)[S_\varepsilon S_\tau - iS_\varepsilon C_\tau]}{(b+1)\,(\frac{c^2a^4}{(1+a)^2} + \omega^{*2})S_\varepsilon^2}\Bigg]
\end{aligned}$$

$$= \mathrm{Re}\Bigg[\frac{\frac{c^2a^4}{(1+a)^2}}{\omega^{*2}(\frac{c^2a^4}{(1+a)^2}+\omega^{*2})} - \frac{\varepsilon}{\omega^*}\cdot\frac{C_\varepsilon}{S_\varepsilon} + \varepsilon\cdot\frac{[\frac{ca^2}{1+a}\cdot\frac{ca^2-b(a+2)}{1+a}+2\omega^{*2}]S_\varepsilon S_\tau + \frac{ca^2+b(a+2)}{1+a}\omega^* S_\varepsilon C_\tau}{(b+1)\left[(\frac{c^2a^4}{(1+a)^2}+\omega^{*2})\right]S_\varepsilon^2}\Bigg],$$

where $C_\varepsilon = \cos(\varepsilon\omega^*)$, $C_\tau = \cos(\tau^*\omega^*)$, $S_\varepsilon = \sin(\varepsilon\omega^*)$, and $S_\tau = \sin(\tau^*\omega^*)$.

Since

$$S_\varepsilon S_\tau = \frac{1}{(1+a)^2}\cdot\frac{\varepsilon\omega^{*2}\left[ca^2\left(ca^2-b\right)+(1+a)^2\omega^{*2}\right]}{(b+1)\left[\frac{c^2a^4}{(1+a)^2}+\omega^{*2}\right]}, \tag{2.23}$$

$$S_\varepsilon C_\tau = \frac{1}{(1+a)^2}\cdot\frac{\varepsilon\omega^* b\left[c^2a^4+(1+a)(2+a)\omega^{*2}\right]}{(b+1)\left[\frac{c^2a^4}{(1+a)^2}+\omega^{*2}\right]}, \tag{2.24}$$

we can further obtain

$$\begin{aligned}
\mathrm{Re}\left[\left(\frac{d\lambda}{d\tau}\right)^{-1}\Big|_{\tau=\tau^*}\right] =& \frac{\frac{c^2a^4}{(1+a)^2}}{\omega^{*2}\left[\frac{c^2a^4}{(1+a)^2}+\omega^{*2}\right]} - \frac{\varepsilon}{\omega^*}\cot(\varepsilon\omega^*) + \frac{\varepsilon}{(b+1)\left[\frac{c^2a^4}{(1+a)^2}+\omega^{*2}\right]S_\varepsilon^2} \\
&\cdot\Bigg[\frac{\left[\frac{ca^2-b(a+2)}{1+a}\cdot\frac{ca^2}{1+a}+2\omega^{*2}\right]\cdot\varepsilon\omega^{*2}\left[ca^2\left(ca^2-b\right)+(1+a)^2\omega^{*2}\right]}{(b+1)\left[c^2a^4+(1+a)^2\omega^{*2}\right]} \\
&+\frac{\frac{ca^2+b(a+2)}{1+a}\omega^*\cdot\varepsilon\omega^* b\left[c^2a^4+(1+a)(2+a)\omega^{*2}\right]}{(b+1)\left[c^2a^4+(1+a)^2\omega^{*2}\right]}\Bigg] \\
=& \frac{\frac{c^2a^4}{(1+a)^2}}{\omega^{*2}\left[\frac{c^2a^4}{(1+a)^2}+\omega^{*2}\right]} - \frac{\varepsilon}{\omega^*}\cot(\varepsilon\omega^*) \\
&+\frac{1}{(1+a)^2}\frac{\varepsilon^2\omega^{*2}[2(1+a)^2\omega^{*4}+A\omega^{*2}+B]}{(b+1)^2\left[\frac{c^2a^4}{(1+a)^2}+\omega^{*2}\right]^2\sin^2(\varepsilon\omega^*)},
\end{aligned}$$

where

$$A = (a^2c-b)^2+2a^4c^2+b^2(a+3)(a+1), \qquad B = \frac{a^4c^2[(a^2c-b)^2+b^2(1+a)(3+a)]}{(1+a)^2}.$$

Clearly $A > 0$ and $B > 0$. Moreover, for $\omega^* \in (\frac{\pi}{2\varepsilon}, \frac{\pi}{\varepsilon})$, we have $\cot(\varepsilon\omega^*) < 0$. Consequently,

$$\frac{d\,\mathrm{Re}(\lambda)}{d\tau}\Big|_{\tau=\tau^*} > 0.$$

The transversality condition is therefore satisfied, which implies that a Hopf bifurcation occurs as τ passes through the critical value τ^*. The proof is complete. □

Remark 2.1. *Theorem 2.2 shows that, under the parameter conditions of Theorem 2.2, the positive equilibrium loses its stability through a Hopf bifurcation as the delay center τ crosses the critical*

value τ^*. The resulting sustained oscillations are thus induced purely by the delay effect, since the equilibrium itself is independent of the delay parameters. This highlights the essential role of time delays in shaping the dynamics of the modified Brusselator system (1.2).

Remark 2.2. *The threshold ε_0 in Theorem 2.2 is obtained from a sufficient sign condition ensuring the existence and uniqueness of a positive root of $p(\omega)$ in the interval $\left(\frac{\pi}{2\varepsilon}, \frac{\pi}{\varepsilon}\right)$. Hence, the requirement $\varepsilon > \varepsilon_0$ is a* sufficient but not necessary *condition for the existence of Hopf bifurcation with respect to the delay center τ. When $\varepsilon \le \varepsilon_0$, the theorem does not exclude the possibility of Hopf bifurcation; rather, the analytical criterion becomes inconclusive. In such cases, the existence of Hopf points can still be examined numerically by solving the characteristic equation $F(i\omega) = 0$ directly.*

For the parameter set used in the numerical simulations ($a = 2.5$, $b = 1.2$, $c = 2.0$), the computed value is $\varepsilon_0 = 2.0484$. Since our simulations are performed in the admissible region $0 < \varepsilon < \tau < 0.5$, the sufficient condition $\varepsilon > \varepsilon_0$ is not satisfied. Therefore, the Hopf curves reported in Section 3 are obtained via numerical solution of the characteristic equation, which complements the theoretical results.

2.2.2. Hopf bifurcation with respect to the delay width ε

Theorem 2.2 shows that the distribution width ε significantly influences the stability of the equilibrium via Hopf bifurcation in τ. This leads to a natural question: Can ε itself serve as a bifurcation parameter and induce oscillatory dynamics?

In this subsection, we answer this question by investigating Hopf bifurcation with respect to ε while keeping τ fixed. We show that, under suitable conditions, increasing ε may also trigger a Hopf bifurcation, giving rise to a second bifurcation branch that is fundamentally associated with the distributed nature of the delay.

From (2.17) and (2.18), define the function

$$\begin{aligned} G(\omega, \varepsilon) = {} & (1+a)^2\omega^4 + [b^2(1+a)(3+a) + (a^2c - b)^2]\omega^2 + a^4b^2c^2 \\ & - \frac{(b+1)^2[c^2a^4 + (1+a)^2\omega^2]}{\varepsilon^2\omega^2} \sin^2(\omega\varepsilon). \end{aligned} \tag{2.25}$$

Consider the implicit relation $G(\omega, \varepsilon) = 0$. Differentiating with respect to ε yields

$$\frac{d\omega}{d\varepsilon} = -\frac{\partial G/\partial\varepsilon}{\partial G/\partial\omega},$$

where

$$\frac{\partial G}{\partial\varepsilon} = -(b+1)^2[c^2a^4 + (1+a)^2\omega^2]\left(\frac{\sin(2\omega\varepsilon)}{\omega\varepsilon^2} - \frac{2\sin^2(\omega\varepsilon)}{\omega^2\varepsilon^3}\right),$$

$$\begin{aligned} \frac{\partial G}{\partial\omega} = {} & 4(1+a)^2\omega^3 + 2[b^2(1+a)(3+a) + (a^2c - b)^2]\omega \\ & - \frac{(b+1)^2}{\varepsilon^2}\left[-\frac{2c^2a^4}{\omega^3}\sin^2(\omega\varepsilon) + \left(\frac{c^2a^4}{\omega^2} + (1+a)^2\right)\varepsilon\sin(2\omega\varepsilon)\right]. \end{aligned}$$

For $\omega \in (\frac{\pi}{2\varepsilon}, \frac{\pi}{\varepsilon})$, we have $\sin(2\omega\varepsilon) < 0$, which implies

$$\frac{\partial G}{\partial\varepsilon} > 0, \qquad \frac{\partial G}{\partial\omega} > 0. \tag{2.26}$$

Consequently,

$$\frac{d\omega}{d\varepsilon} < 0.$$

Next, we compute $\frac{d\tau}{d\varepsilon}$ by the chain rule:

$$\frac{d\tau}{d\varepsilon} = \frac{d\tau}{d\omega} \cdot \frac{d\omega}{d\varepsilon}.$$

Let

$$Q = \frac{b[c^2a^4 + (1+a)^2\omega^2]^2}{\omega[ca^2(ca^2-b) + (1+a)^2\omega^2]},$$

then $\tau = \frac{1}{\omega}\text{arccot}Q$, and hence

$$\frac{d\tau}{d\omega} = -\frac{1}{\omega^2}\text{arccot}Q - \frac{1}{\omega(1+Q^2)}\frac{dQ}{d\omega} = -\frac{\tau}{\omega} - \frac{1}{\omega(1+Q^2)}\frac{dQ}{d\omega}. \tag{2.27}$$

Write $Q = N/D$, where

$$N = b[c^2a^4 + (1+a)^2\omega^2]^2, \qquad D = \omega[ca^2(ca^2-b) + (1+a)^2\omega^2].$$

Then,

$$\frac{dQ}{d\omega} = \frac{N'D - ND'}{D^2}.$$

A direct calculation yields

$$N'D - ND' = b(1+a)^2H(\omega^2),$$

where

$$H(x) \triangleq A_3x^3 - A_2x^2 - A_1x + A_0,$$

with

$$A_3 = (1+a)^4, \quad A_2 = ca^2(1+a)^2(ca^2-3b), \quad A_1 = c^3a^6(ca^2+2b), \quad A_0 = \frac{c^5a^{10}}{(1+a)^2}(ca^2-b).$$

If $ca^2 > b$, then $A_0 > 0$. Thus,

$$H(0) = A_0 = \frac{c^5a^{10}}{(1+a)^2}(ca^2-b) > 0.$$

In addition,

$$H'(x) = 3A_3x^2 - 2A_2x - A_1, \qquad H'(0) = -A_1 < 0.$$

Obviously, $H'(x) = 0$ admits a unique positive root

$$x_2 = \frac{A_2 + \sqrt{A_2^2 + 3A_1A_3}}{3A_3},$$

and $H(x)$ is decreasing on $[0, x_2]$ and increasing on $[x_2, \infty)$. If $H(x_2) > 0$, then $H(x) > 0$ for all $x > 0$ and $\frac{dQ}{d\omega} > 0$ for all $\omega > 0$.

Since $\dfrac{d\omega}{d\varepsilon} < 0$ and

$$\frac{d\tau}{d\omega} = -\frac{\tau}{\omega} - \frac{1}{\omega(1+Q^2)}\frac{dQ}{d\omega}, \quad \omega > 0, \tag{2.28}$$

we conclude that

$$\frac{d\tau}{d\varepsilon} > 0 \quad \text{for all } \omega \in \left(\frac{\pi}{2\varepsilon}, \frac{\pi}{\varepsilon}\right), \tag{2.29}$$

which shows that τ is a strictly increasing function of ε.

From (2.17) and (2.28), we obtain the asymptotic behaviors: $\omega \to 0^+$ as $\tau \to \infty$, and $\omega \to \infty$ as $\tau \to 0^+$. Thus, for any given $\hat{\tau} > \tau^*$, there exists a unique $\hat{\varepsilon}$ such that equation $G(\omega, \varepsilon) = 0$ admits a unique solution:

$$\omega_{\hat{\varepsilon}} \in \left(\frac{\pi}{2\varepsilon}, \frac{\pi}{\varepsilon}\right).$$

The following theorem establishes the existence of Hopf bifurcation with respect to ε.

Theorem 2.3. *Assume $ca^2 > b$ and $H(x_2) > 0$. Fix $\hat{\tau} > \max\{\tau^*, \frac{1+a}{ca^2}\}$, where τ^* is given in Theorem 2.2. Then there exists a unique critical value $\hat{\varepsilon}$ satisfying system* (2.17)*. As ε decreases from values larger than $\hat{\varepsilon}$ to $\hat{\varepsilon}$, system* (1.2) *undergoes a Hopf bifurcation at $\varepsilon = \hat{\varepsilon}$. In particular, the equilibrium (X^*, Y^*) loses its stability and a family of periodic solutions bifurcates from it.*

Proof. It suffices to verify that the conjugate purely imaginary roots $\lambda = i\hat{\omega}$ of characteristic equation (2.5) satisfy the transversality condition:

$$\frac{d\,\mathrm{Re}(\lambda)}{d\varepsilon}\Big|_{\varepsilon=\hat{\varepsilon}} < 0.$$

This condition implies that the real part of the characteristic root turns positive as ε decreases, resulting in the loss of system stability.

Rewrite the characteristic equation (2.5) as

$$2\varepsilon\lambda^3 + 2\varepsilon \cdot \frac{1}{1+a}(ca^2 - ab - 2b)\lambda^2 + 2\varepsilon\Big(-\frac{ca^2 b}{1+a}\Big)\lambda + \Big[(b+1)\lambda + \frac{ca^2}{1+a}(b+1)\Big](e^{(-\tau+\varepsilon)\lambda} - e^{(-\tau-\varepsilon)\lambda}) = 0.$$

Let

$$\alpha = \frac{1}{1+a}(ca^2 - ab - 2b), \quad \beta = -\frac{ca^2 b}{1+a} < 0, \quad \gamma = b + 1 > 0, \quad \eta = \frac{ca^2}{1+a}(b+1) > 0.$$

Then, the characteristic equation becomes

$$\mathcal{F}(\lambda, \varepsilon) = 2\varepsilon\lambda^3 + 2\varepsilon\alpha\lambda^2 + 2\varepsilon\beta\lambda + (\gamma\lambda + \eta)(e^{(-\tau+\varepsilon)\lambda} - e^{(-\tau-\varepsilon)\lambda}) = 0. \tag{2.30}$$

Differentiating with respect to ε yields

$$\begin{aligned}\left(\frac{d\lambda}{d\varepsilon}\right)^{-1} &= -\frac{\frac{\partial \mathcal{F}}{\partial \lambda}}{\frac{\partial \mathcal{F}}{\partial \varepsilon}} \\ &= -\frac{6\varepsilon\lambda^2 + 4\varepsilon\alpha\lambda + 2\varepsilon\beta + \gamma \cdot (E_1 - E_2) + (\gamma\lambda + \eta)[E_1 \cdot (-\tau + \varepsilon) - E_2 \cdot (-\tau - \varepsilon)]}{2\lambda^3 + 2\alpha\lambda^2 + 2\lambda\beta + (\gamma\lambda + \eta)(E_1 \cdot \lambda + E_2 \cdot \lambda)} \\ &= -\frac{6\varepsilon\lambda^2 + 4\varepsilon\alpha\lambda + 2\varepsilon\beta + [\gamma - (\gamma\lambda + \eta)(\tau - \varepsilon)]E_1 - [\gamma - (\gamma\lambda + \eta)(\tau + \varepsilon)]E_2}{2\lambda^3 + 2\alpha\lambda^2 + 2\lambda\beta + (\gamma\lambda + \eta)\lambda(E_1 + E_2)},\end{aligned} \tag{2.31}$$

where $E_1 = e^{(-\tau+\varepsilon)\lambda}$ and $E_2 = e^{(-\tau-\varepsilon)\lambda}$.

Let $(\frac{d\lambda}{d\varepsilon})^{-1} = -\frac{R}{S}$, where

$$\begin{aligned} R &= 6\varepsilon\lambda^2 + 4\varepsilon\alpha\lambda + 2\varepsilon\beta \\ &\quad + [\gamma - (\gamma\lambda + \eta)(\tau - \varepsilon)]e^{(-\tau+\varepsilon)\lambda} - [\gamma - (\gamma\lambda + \eta)(\tau + \varepsilon)]e^{(-\tau-\varepsilon)\lambda}, \\ S &= 2\lambda^3 + 2\alpha\lambda^2 + 2\beta\lambda + (\gamma\lambda + \eta)\lambda(e^{(-\tau+\varepsilon)\lambda} + e^{(-\tau-\varepsilon)\lambda}). \end{aligned}$$

Substituting $\lambda = i\hat{\omega}$ into R and S, we obtain

$$\begin{aligned} R &= -6\hat{\varepsilon}\hat{\omega}^2 + 4i\hat{\varepsilon}\alpha\hat{\omega} + 2\hat{\varepsilon}\beta \\ &\quad + [\gamma - (i\gamma\hat{\omega} + \eta)(\hat{\tau} - \hat{\varepsilon})]e^{(-\hat{\tau}+\hat{\varepsilon})i\hat{\omega}} - [\gamma - (i\gamma\hat{\omega} + \eta)(\hat{\tau} + \hat{\varepsilon})]e^{(-\hat{\tau}-\hat{\varepsilon})i\hat{\omega}}, \\ S &= 2(i\hat{\omega})^3 + 2\alpha(i\hat{\omega})^2 + 2\beta(i\hat{\omega}) + (i\gamma\hat{\omega} + \eta)i\hat{\omega}(e^{(-\hat{\tau}+\hat{\varepsilon})i\hat{\omega}} + e^{(-\hat{\tau}-\hat{\varepsilon})i\hat{\omega}}). \end{aligned}$$

Now, the transversality condition is determined by the sign of

$$\frac{d\,\mathrm{Re}(\lambda)}{d\varepsilon}\Big|_{\varepsilon=\hat{\varepsilon}} = \mathrm{Re}\left(\frac{d\lambda}{d\varepsilon}\right)\Big|_{\varepsilon=\hat{\varepsilon}} = \mathrm{Re}\left(-\frac{S}{R}\right) = -\frac{\mathrm{Re}(R)\mathrm{Re}(S) + \mathrm{Im}(R)\mathrm{Im}(S)}{|R|^2}.$$

Hence, it suffices to check the sign of the numerator:

$$\Phi := -(\mathrm{Re}(R)\mathrm{Re}(S) + \mathrm{Im}(R)\mathrm{Im}(S)). \tag{2.32}$$

After substituting the expressions for $\mathrm{Re}(R)$, $\mathrm{Im}(R)$, $\mathrm{Re}(S)$, and $\mathrm{Im}(S)$ and performing algebraic simplifications, we obtain

$$\begin{aligned} \Phi &= -4\alpha\hat{\varepsilon}\hat{\omega}^4 + 4\alpha\beta\hat{\varepsilon}\hat{\omega}^2 + [-4\gamma\hat{\tau}\hat{\omega}^4 + 4\alpha(\gamma - \eta\hat{\tau})\hat{\omega}^2 + 4\beta\gamma\hat{\tau}\hat{\omega}^2]\sin(\hat{\tau}\hat{\omega})\sin(\hat{\varepsilon}\hat{\omega}) \\ &\quad + [4\alpha\gamma\hat{\tau}\hat{\omega}^3 + 4(\gamma - \eta\hat{\tau})\hat{\omega}^3 - 4\beta(\gamma - \eta\hat{\tau})\hat{\omega}]\cos(\hat{\tau}\hat{\omega})\sin(\hat{\varepsilon}\hat{\omega}) \\ &\quad - (8\gamma\hat{\varepsilon}\hat{\omega}^4 + 4\alpha\eta\hat{\varepsilon}\hat{\omega}^2)\cos(\hat{\tau}\hat{\omega})\sin(\hat{\varepsilon}\hat{\omega}) + (8\eta\hat{\varepsilon}\hat{\omega}^3 - 4\alpha\gamma\hat{\varepsilon}\hat{\omega}^3)\sin(\hat{\tau}\hat{\omega})\cos(\hat{\varepsilon}\hat{\omega}) \\ &\quad + 4\gamma^2\hat{\omega}^3\sin(\hat{\varepsilon}\hat{\omega})\cos(\hat{\varepsilon}\hat{\omega}) - 4(\gamma - \eta\hat{\tau})\eta\hat{\omega}\sin(\hat{\varepsilon}\hat{\omega})\cos(\hat{\varepsilon}\hat{\omega}). \end{aligned}$$

When $\hat{\tau} > \gamma/\eta = \frac{1+a}{ca^2}$, we can further simplify Φ by using the previously defined relations between Δ_1 and Δ_2 as follows:

$$\begin{aligned} \Phi &= -4\alpha\hat{\varepsilon}\hat{\omega}^4 + 4\alpha\beta\hat{\varepsilon}\hat{\omega}^2 - [4\gamma\hat{\tau}\hat{\omega}^4 - 4\alpha(\gamma - \eta\hat{\tau})\hat{\omega}^2 + 4\beta\gamma\hat{\tau}\hat{\omega}^2] \cdot \frac{\hat{\varepsilon}\hat{\omega}^2[ca^2(ca^2 - b) + (1+a)^2\hat{\omega}^2]}{(b+1)[c^2a^4 + (1+a)^2\hat{\omega}^2]} \\ &\quad + [4\alpha\gamma\hat{\tau}\hat{\omega}^3 + 4(\gamma - \eta\hat{\tau})\hat{\omega}^3 - 4\beta(\gamma - \eta\hat{\tau})\hat{\omega}] \cdot \frac{\hat{\varepsilon}\hat{\omega}b[c^2a^4 + (1+a)(2+a)\hat{\omega}^2]}{(b+1)[c^2a^4 + (1+a)^2\hat{\omega}^2]} \\ &\quad - (8\gamma\hat{\varepsilon}\hat{\omega}^3 + 4\alpha\eta\hat{\varepsilon}\hat{\omega}^2)\frac{\hat{\varepsilon}\hat{\omega}b[c^2a^4 + (1+a)(2+a)\hat{\omega}^2]}{(b+1)[c^2a^4 + (1+a^2)\hat{\omega}^2]} \cdot \cot(\hat{\omega}\hat{\varepsilon}) \\ &\quad + (8\eta\hat{\varepsilon}\hat{\omega}^3 - 4a\gamma\hat{\varepsilon}\hat{\omega}^3)\frac{\hat{\varepsilon}\hat{\omega}^2[ca^2(ca^2 - b) + (1+a)^2\hat{\omega}^2]}{(b+1)[c^2a^4 + (1+a)^2\hat{\omega}^2]} \cdot \cot(\hat{\omega}\hat{\varepsilon}) \\ &\quad + 4\gamma^2\hat{\tau}\hat{\omega}^3\sin\hat{\varepsilon}\hat{\omega}\cos\hat{\varepsilon}\hat{\omega} - 4(\gamma - \eta\hat{\tau})\eta\hat{\omega}\sin\hat{\varepsilon}\hat{\omega}\cos\hat{\varepsilon}\hat{\omega} \\ &= -4\alpha\hat{\varepsilon}\hat{\omega}^2(\hat{\omega}^2 - \beta) + (\hat{\omega}^2 - \beta)(4\alpha\gamma^2\hat{\varepsilon}\hat{\omega}^4 + 4\alpha\eta^2\hat{\varepsilon}\hat{\omega}^2)\frac{\hat{\varepsilon}\hat{\omega}\cot(\hat{\varepsilon}\hat{\omega})}{\eta^2 + \gamma^2\hat{\omega}^2} \end{aligned}$$

$$- 4\gamma^2\hat{\tau}\hat{\omega}^7 - [4\eta(\eta\hat{\tau} - \gamma) + 4\gamma^2\hat{\tau}(\alpha^2 - 2\beta)]\hat{\omega}^5 - [4\beta^2\gamma^2 + 4\eta(\eta\hat{\tau} - \gamma)(\alpha^2 - 2\beta)]\hat{\omega}^3$$
$$- 4\beta^2\eta(\eta\hat{\tau} - \gamma)\hat{\omega} + [2\gamma^2\hat{\tau}\hat{\omega}^3 + 2\eta\hat{\omega}(\eta\hat{\tau} - \gamma)]\sin(2\hat{\varepsilon}\hat{\omega}).$$

Since $\hat{\varepsilon}\hat{\omega} \in (\frac{\pi}{2}, \pi)$ implies $\cot(\hat{\omega}\hat{\varepsilon}) < 0$ and $\sin(2\hat{\varepsilon}\hat{\omega}) < 0$, we can verify that under the assumptions of Theorem 2.3, all terms in the above expression are negative, hence $\Phi < 0$. Consequently,

$$\left.\frac{d\,\mathrm{Re}(\lambda)}{d\varepsilon}\right|_{\varepsilon=\hat{\varepsilon}} < 0.$$

Therefore, the transversality condition is satisfied, and a Hopf bifurcation occurs as ε decreases through $\hat{\varepsilon}$. The proof is complete. □

Remark 2.3. *Theorem 2.3 demonstrates that the distributed delay width ε can also serve as a bifurcation parameter, complementing the previously established Hopf bifurcation with respect to the mean delay τ. This highlights an important dual role of the delay distribution: While the delay center τ measures the average time lag, the distribution width ε controls the degree of temporal dispersion. The fact that both parameters can induce Hopf bifurcations underscores the richness of the delay-induced dynamics in the modified Brusselator system* (1.2).

3. Numerical simulations

In this section, we perform numerical simulations to illustrate and complement the theoretical results derived in Section 2. The reaction parameters are fixed throughout as

$$a = 2.5, \qquad b = 1.2, \qquad c = 2.0,$$

and the admissible delay parameter region $0 < \varepsilon < \tau < 0.5$ is considered. For the chosen reaction constants, the system possesses the unique positive equilibrium

$$E^* = (X^*, Y^*) = \left(a,\ \frac{(1+a)b}{ca}\right) = (2.5,\ 0.84).$$

3.1. Numerical methodology

To simulate the distributed-delay system, the sub-interval delay operator

$$L(X_t) = \frac{1}{2\varepsilon}\int_{-\tau-\varepsilon}^{-\tau+\varepsilon} X(t+\theta)\,d\theta$$

is approximated numerically by discretizing the integral over its finite support interval. Specifically, the integration interval $[-\tau-\varepsilon, -\tau+\varepsilon]$ is partitioned into sufficiently fine subintervals, and the integral is evaluated using a composite quadrature rule.

This approximation transforms the original distributed-delay system into a system of ordinary differential equations coupled with discretized delay states. The resulting finite-dimensional system is then integrated using a standard explicit Runge-Kutta scheme.

Time integration is performed over sufficiently long intervals to eliminate transient dynamics. To distinguish between convergence to equilibrium and sustained oscillatory behavior, the long-term maxima and minima of $X(t)$ and $Y(t)$ are extracted after discarding an initial transient window.

For the computation of Hopf bifurcation curves, the characteristic equation is separated into its real and imaginary parts. The resulting nonlinear algebraic system is solved numerically for (ω, τ) or (ω, ε) using a root-finding procedure. Parameter continuation is then employed to trace the bifurcation curves in the (τ, ε)-plane.

3.2. Numerical results

To verify the local asymptotic stability stated in Theorem 2.1, we take $\tau = 0.25$ and $\varepsilon = 0.1$, which satisfy conditions (2.1) and (2.2). Four distinct constant initial histories are imposed for $t \in [-\tau - \varepsilon, 0]$:

$$(u(t), v(t)) \equiv (X_0, Y_0) = (1.40, 0.40),\ (0.50, 1.30),\ (3.90, 1.50),\ (2.75, 0.55).$$

Figure 1(a) depicts the temporal evolutions of $X(t)$ and $Y(t)$. Although the transient responses differ considerably, exhibiting overshoots and damped oscillations depending on the initial condition, all trajectories converge to the steady state (X^*, Y^*). Figure 1(b) shows the corresponding phase-plane trajectories, which spiral or curve toward E^* from different regions of the phase plane and ultimately converge to the equilibrium. These simulations confirm that for sufficiently small τ and ε, the positive equilibrium is locally asymptotically stable and robust with respect to initial perturbations. In particular, the distributed delay does not destabilize the equilibrium in this parameter regime, thereby providing numerical support for the theoretical stability conditions established in Theorem 2.1.

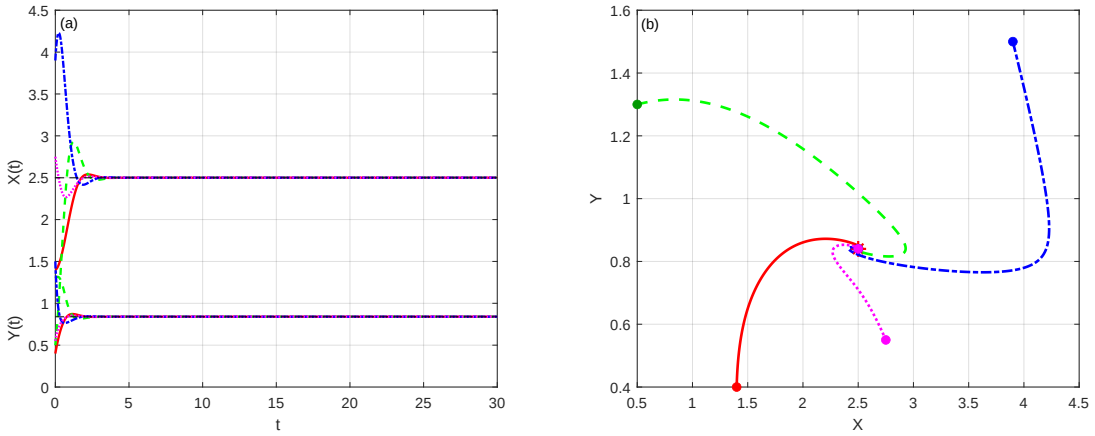

Figure 1. Stability of the positive equilibrium $E^* = (X^*, Y^*)$ of system (1.2). (a) Time evolutions of $X(t)$ and $Y(t)$ for several different initial conditions. (b) Corresponding phase-plane trajectories illustrating convergence toward E^*.

Keeping the reaction parameters fixed at $a = 2.5$, $b = 1.2$, and $c = 2.0$, we numerically compute the Hopf bifurcation curve $\tau = \tau^*(\varepsilon)$ in the (τ, ε)-plane, as predicted by Theorem 2.2 (see Figure 2). In the numerical computations, the delay parameters are restricted to the region $0 \le \varepsilon \le \tau \le 0.5$, which ensures that the sub-interval distributed delay operator is well defined. The line $\tau = \varepsilon$ (red dashed line in the figure) separates the admissible parameter region from the invalid one. The blue solid curve marks the critical boundary across which a pair of complex conjugate eigenvalues crosses the imaginary axis, separating stable from unstable dynamics. The green region left of the curve denotes local asymptotic stability of the positive equilibrium E^*, and the light-blue region to the right of it indicates instability with Hopf bifurcation-induced oscillatory solutions.

This diagram highlights the intricate interplay between the delay center τ and the distribution width ε in governing stability. Crossing the Hopf boundary from the stable to the unstable region can be achieved by increasing τ while holding some ε fixed. Notably, for some fixed τ, varying ε can also induce stability switches. This indicates that both delay characteristics jointly determine the system's stability. Such a two-parameter stability structure illustrates the richer dynamics introduced by distributed delays, which is absent in classical discrete delay Brusselator models.

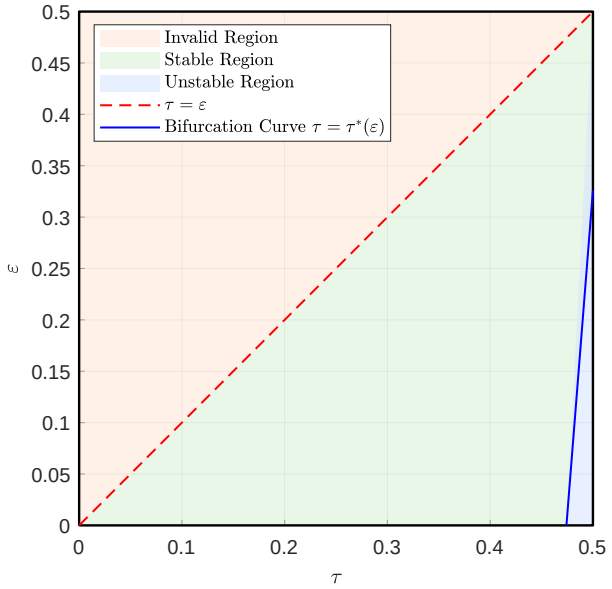

Figure 2. Hopf bifurcation boundary and stability regions in the $\tau - \varepsilon$ parameter plane.

The bifurcation diagrams in Figure 3 correspond directly to one-dimensional cross-sections of the two-parameter Hopf boundary shown in Figure 2. Panels (a–c) represent a horizontal slice obtained by fixing the delay width at $\varepsilon = 0.01$ and varying the delay center τ. Along this slice, the solution remains stable for parameter values to the left of the Hopf curve, while periodic oscillations emerge once the curve is crossed. This behavior is fully consistent with the theoretical prediction of Theorem 2.2.

Panels (d–f) show a vertical slice with fixed $\tau = 0.5$ and varying distribution width ε. In this case, the system crosses the Hopf curve in the opposite direction. For small ε, the parameters lie in the unstable region, producing sustained oscillations. Increasing ε moves the system into the stable region, where the amplitude decays to zero and the equilibrium regains stability. This agrees with the stabilizing effect of the distribution width predicted by Theorem 2.3.

To further validate the bifurcation structure and stability regions delineated in Figure 3, we select three representative pairs of delay parameters (τ, ε) and simulate the asymptotic dynamics of model (1.2). The results are displayed using time series and phase-plane trajectories.

For the parameter pair $(\tau, \varepsilon) = (0.15, 0.01)$ (Figure 4), which lies inside the stable region of Figure 2, numerical simulations show that the state variables $X(t)$ and $Y(t)$ converge rapidly to the unique positive equilibrium. In the phase plane, trajectories spiral or curve directly toward the equilibrium. This confirms the bifurcation diagram prediction that the equilibrium remains stable for sufficiently small τ and ε, indicating that the delay strength here is insufficient to destabilize the steady state.

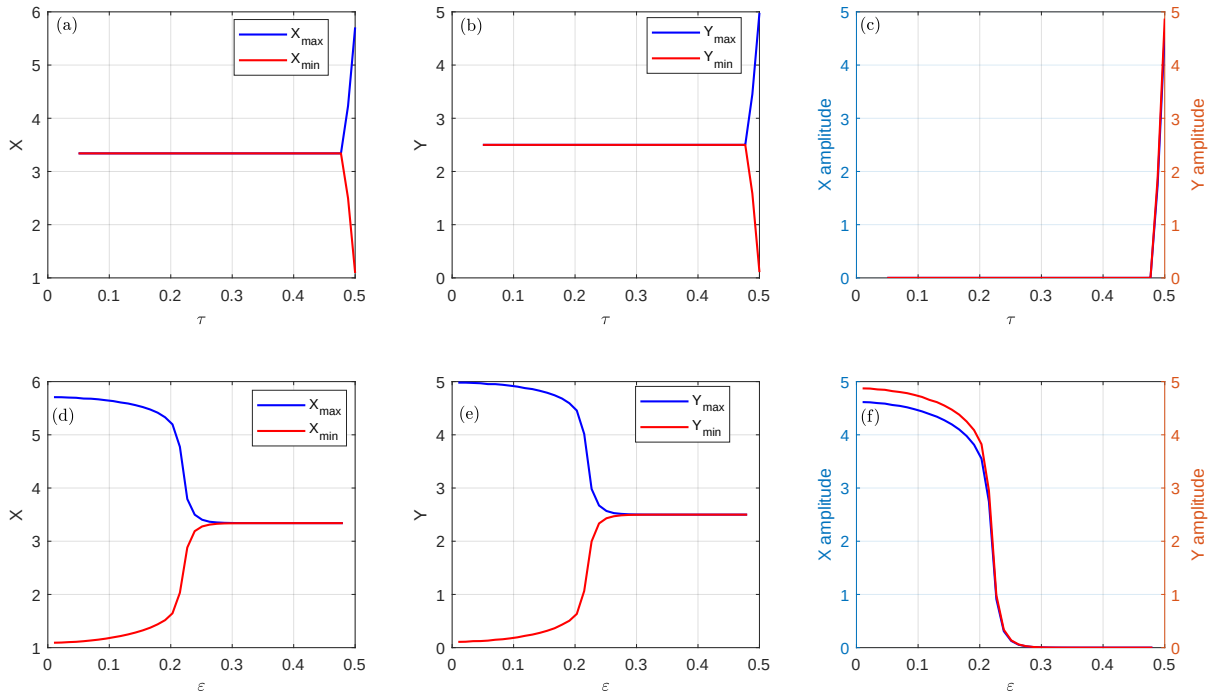

Figure 3. Bifurcation diagrams of system (1.2) with respect to the delay parameters. (a–c) Variation with respect to the delay center τ for fixed $\varepsilon = 0.01$: (a) $X_{\max}$ and $X_{\min}$ versus τ; (b) $Y_{\max}$ and $Y_{\min}$ versus τ; (c) oscillation amplitudes of $X(t)$ and $Y(t)$ versus τ. (d–f) Variation with respect to the delay width ε for fixed $\tau = 0.5$: (d) $X_{\max}$ and $X_{\min}$ versus ε; (e) $Y_{\max}$ and $Y_{\min}$ versus ε; (f) oscillation amplitudes of $X(t)$ and $Y(t)$ versus ε.

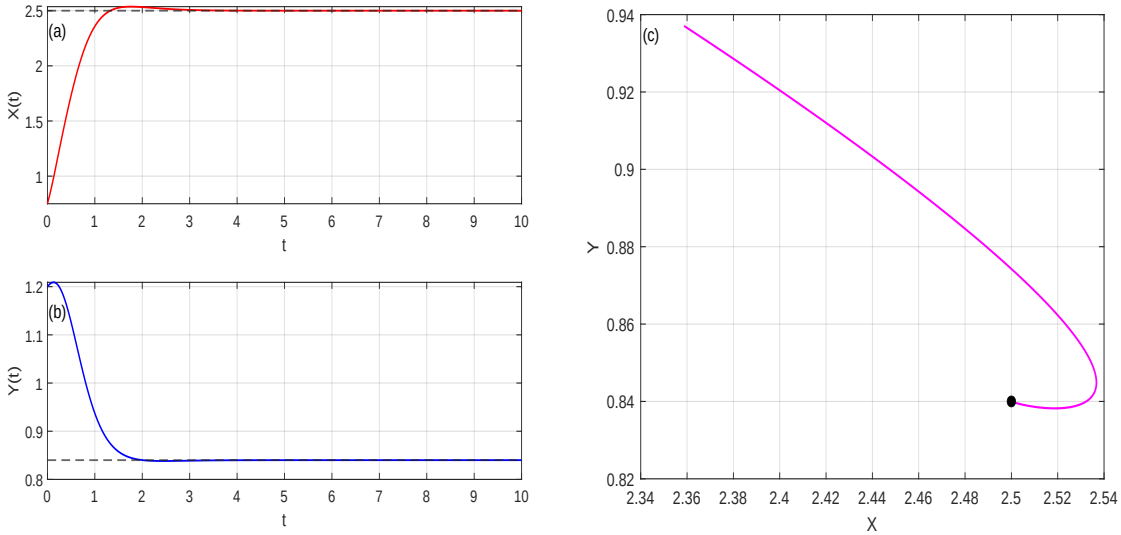

Figure 4. Asymptotic behavior of system (1.2) for $(\tau, \varepsilon) = (0.15, 0.01)$. (a) Time evolution of $X(t)$. (b) Time evolution of $Y(t)$. (c) Phase-plane trajectory converging to the positive equilibrium E^*.

For $(\tau, \varepsilon) = (0.5, 0.01)$ (Figure 5), this point lies in the unstable region beyond the Hopf curve in Figure 2. After a brief transient, $X(t)$ and $Y(t)$ quickly enter a state of sustained periodic oscillation with constant amplitude and period. The corresponding trajectory in the phase plane forms a closed limit cycle, enclosing the now-unstable equilibrium point. These results confirm a Hopf bifurcation has occurred in this parameter regime, where the equilibrium loses stability and a stable periodic solution emerges. This confirms the existence of the "oscillatory region" in the bifurcation diagram.

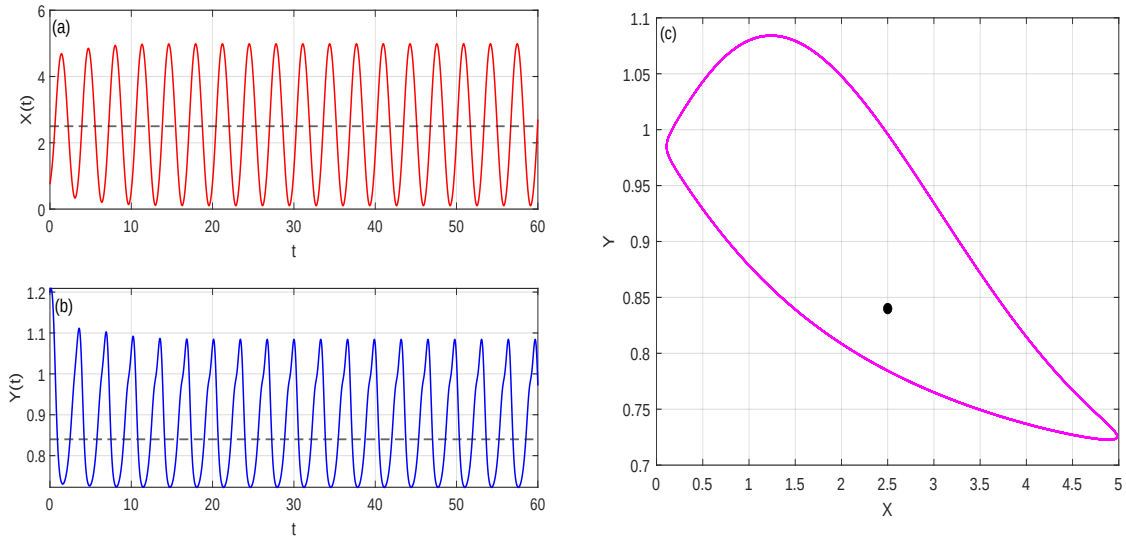

Figure 5. Asymptotic periodic behavior of system (1.2) for $(\tau, \varepsilon) = (0.50, 0.01)$, corresponding to a parameter pair beyond the Hopf bifurcation threshold. (a) Time evolution of $X(t)$ showing sustained oscillations. (b) Time evolution of $Y(t)$. (c) Corresponding phase-plane trajectory illustrating the emergence of a stable limit cycle around the equilibrium E^*.

For $(\tau, \varepsilon) = (0.5, 0.48)$ (Figure 6), where τ remains large but ε is significantly increased, the oscillatory behavior is markedly suppressed. Simulations show that after an initial phase of damped oscillations, $X(t)$ and $Y(t)$ reconverge to the equilibrium. In the phase plane, trajectories spiral inward and settle at the equilibrium. This result aligns with the trend in Figure 3, where the oscillation amplitude decays to zero as ε increases. It demonstrates that broadening the delay distribution effectively counteracts the oscillatory instability induced by a concentrated delay.

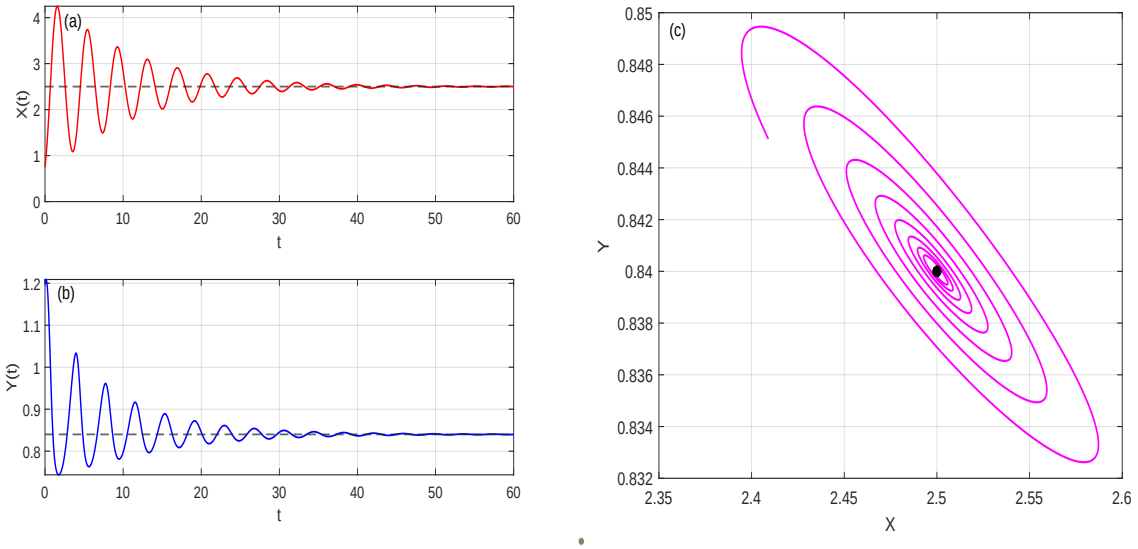

Figure 6. Asymptotic behavior of system (1.2) for $(\tau, \varepsilon) = (0.50, 0.48)$. (a) Time evolution of $X(t)$. (b) Time evolution of $Y(t)$. (c) Phase-plane trajectory converging to the positive equilibrium E^*.

Together, Figures 3–6 demonstrate directly through trajectory level simulations the bifurcation structure identified in Figures 2 and 3: An increase in the delay center τ tends to induce and enhance system oscillations, while an increase in the delay distribution width ε exerts a significant stabilizing effect. From a biological standpoint, this suggests that discrete or narrowly concentrated delays in regulatory pathways are prone to causing unnecessary periodic fluctuations in the system. By spreading the delayed feedback over a broader time window, feedback can be smoothed, oscillations suppressed, and steady state operation of the system maintained.

4. Conclusions

In this paper, we have analyzed a modified Brusselator model equipped with a moderated autocatalytic term and a sub-interval distributed delay that is characterized by a center τ and a width ε. This modification introduces a more realistic representation of delay effects by distributing the delay over a finite time interval rather than assuming a discrete delay. Such a formulation captures more accurately the continuous nature of delay in biological and chemical processes. By varying both the delay center and width, we can better understand the interplay between these two parameters and their individual effects on system dynamics.

Theoretical analysis reveals that the system undergoes a Hopf bifurcation as τ or ε crosses a critical threshold, leading to a transition between a stable equilibrium and sustained periodic oscillations. Numerical simulations confirm both bifurcation scenarios, demonstrating the emergence of oscillatory dynamics that agree with the theoretical predictions.

The study exhibits two interacting delay governed mechanisms: (i) a destabilizing role of τ, which triggers oscillations, and (ii) a stabilizing role of ε, which suppresses oscillations and restores equilibrium stability. These results highlight the essential influence of distributed delays on the stability

and dynamics of Brusselator-modeled chemical and biological systems. They also suggest potential strategies for controlling oscillatory behavior in real world applications.

Future work will explore the effects of nonlinearities, higher-dimensional model extensions, and additional biological or chemical interactions. These factors may further enrich the system's dynamical landscape.

Author contributions

Shouzong Liu: Conceptualization, writing-original draft preparation, supervision, methodology; Tingting Lu: Writing-original draft preparation; Jianing Qin: Writing-review and editing; Yaxin Niu: Writing-review and editing. All authors have read and approved the final version of the manuscript for publication.

Use of Generative-AI tools declaration

The authors declare that they have not used Artificial Intelligence (AI) tools in the creation of this article.

Acknowledgments

This work is supported by Natural Science Foundation of Henan Province (252300420346), Scientific Research Foundation of Graduate School of Xinyan Normal University (2025KYJJ52) and Nanhu Scholars Program for Young Scholars of Xinyang Normal University.

Conflict of interest

The authors declare that they have no competing interests.

References

1. S. Maćešić, Z. Čupić, L. Kolar-Anić, Model of a nonlinear reaction system with autocatalysis and autoinhibition: Stability of dynamic states, *Hem. Ind.*, **66** (2012), 637–646. https://doi.org/10.2298/HEMIND120210034M
2. D. V. Kriukov, J. Huskens, A. S. Y. Wong, Exploring the programmability of autocatalytic chemical reaction networks, *Nat. Commun.*, **15** (2024), 8289. https://doi.org/10.1038/s41467-024-52649-z
3. I. Bashkirtseva, M. Pavletsov, T. Perevalova, L. Ryashko, Mechanisms of stochastic excitement in a nonlinear thermochemical model of autocatalysis, *Nonlinear Dyn.*, **113** (2025), 2199–2213. https://doi.org/10.1007/s11071-024-10335-1
4. T. Erneux, E. Reiss, Brusselator isolas, *SIAM J. Appl. Math.*, **43** (1983), 1240–1246. https://doi.org/10.1137/0143082
5. I. Prigogine, G. Nicolis, Self-organisation in nonequilibrium systems: Towards a dynamics of complexity, In: *Bifurcation analysis*, Dordrecht: Springer, 1985, 3–12. https://doi.org/10.1007/978-94-009-6239-2_1

6. I. R. Epstein, J. A. Pojman, *An introduction to nonlinear chemical dynamics: Oscillations, waves, patterns, and chaos*, Oxford: Oxford University Press, 1998. https://doi.org/10.1093/oso/9780195096705.001.0001
7. J. Zheng, P. Zhang, X. Liu, Global existence and boundedness for an N-dimensional parabolic-elliptic chemotaxis-fluid system with indirect pursuit-evasion, *J. Differ. Equations*, **367** (2023), 199–228. https://doi.org/10.1016/j.jde.2023.04.042
8. K. J. Brown, F. A. Davidson, Global bifurcation in the Brusselator system, *Nonlinear Anal.*, **24** (1995), 1713–1725. https://doi.org/10.1016/0362-546X(94)00218-7
9. H. Y. Alfifi, S. M. Almuaddi, Stability analysis and Hopf bifurcation for the Brusselator reaction-diffusion system with gene expression time delay, *Mathematics*, **12** (2024), 1170. https://doi.org/10.3390/math12081170
10. S. Li, Y. Yang, X. Song, The joint impacts of maturation delay and digestion delay on the dynamics of a predator-prey model, *J. Xinyang Norm. Univ. (Natural Science Edition)*, **38** (2025), 421–427. https://doi.org/10.3969/j.issn.2097-583X.2025.04.007
11. A. M. Alqahtani, Numerical simulation to study the pattern formation of reaction-diffusion Brusselator model arising in triple collision and enzymatic, *J. Math. Chem.*, **56** (2018), 1543–1566. https://doi.org/10.1007/s10910-018-0859-8
12. R. M. Jena, S. Chakraverty, H. Rezazadeh, D. D. Ganji, On the solution of time-fractional dynamical model of Brusselator reaction-diffusion system arising in chemical reactions, *Math. Method Appl. Sci.*, **43** (2020), 3903–3913. https://doi.org/10.1002/mma.6141
13. S. Zhao, P. Yu, W. Jiang, H. Wang, A new mechanism revealed by cross-diffusion-driven instability and double-Hopf bifurcation in the Brusselator system, *J. Nonlinear Sci.*, **35** (2025), 21. https://doi.org/10.1007/s00332-024-10107-6
14. I. Prigogine, R. Lefever, Symmetry breaking instabilities in dissipative systems. II, *J. Chem. Phys.*, **48** (1968), 1695–1700. https://doi.org/10.1063/1.1668896
15. M. Ghergu, V. Radulescu, Turing patterns in general reaction-diffusion systems of Brusselator type, *Commun. Contemp. Math.*, **12** (2010), 661–679. https://doi.org/10.1142/S0219199710003968
16. G. Guo, T. Wei, F. Jia, K. A. Abbakar, Turing instability of periodic solutions for a general Brusselator model with cross-diffusion, *J. Math. Anal. Appl.*, **541** (2025), 128683. https://doi.org/10.1016/j.jmaa.2024.128683
17. Y. Li, Hopf bifurcations in general systems of Brusselator type, *Nonlinear Anal. Real World Appl.*, **28** (2016), 32–47. https://doi.org/10.1016/j.nonrwa.2015.09.004
18. Y. Ji, J. Shen, X. Mao, Pattern formation of Brusselator in the reaction-diffusion system, *Discrete Contin. Dyn. Syst. Ser. S*, **16** (2023), 434–459. https://doi.org/10.3934/dcdss.2022103
19. M. Liao, Q. R. Wang, Stability and bifurcation analysis in a diffusive Brusselator-type system, *Int. J. Bifurcat. Chaos*, **26** (2016), 1650119. https://doi.org/10.1142/S0218127416501194
20. T. Zheng, L. Zhang, Y. Luo, X. Zhou, H. Li, Z. Teng, Stability and Hopf bifurcation of a stage-structured cannibalism model with two delays, *Int. J. Bifurcat. Chaos*, **31** (2021), 2150242. https://doi.org/10.1142/S0218127421502424

21. W. Chen, L. Zhang, N. Wang, Z. Teng, Bifurcation analysis and chaos for a double-strains HIV coinfection model with intracellular delays, saturated incidence and logistic growth, *Math. Comput. Simulation*, **223** (2024), 617–641. https://doi.org/10.1016/j.matcom.2024.04.025

22. B. Song, Y. Zhang, Y. Sang, L. Zhang, Stability and Hopf bifurcation on an immunity delayed HBV/HCV model with intra- and extra-hepatic coinfection and saturation incidence, *Nonlinear Dyn.*, **111** (2023), 14485–14511. https://doi.org/10.1007/s11071-023-08580-x

23. X. Yang, G. Zhang, Turing-Hopf bifurcation of Brusselator model with cross-diffusion and Gene expression time delay, *Int. J. Bifurcat. Chaos*, **35** (2025), 2550159. https://doi.org/10.1142/S0218127425501597

24. Q. Li, B. Liu, Traveling wave fronts to a Mackey-Glass model involving distinct delays in diffusion term and birth function, *Math. Method Appl. Sci.*, **48** (2025), 15549–15558. https://doi.org/10.1002/mma.11109

25. Y. Lv, Z. Liu, Turing-Hopf bifurcation analysis and normal form of a diffusive Brusselator model with gene expression time delay, *Chaos Soliton Fract.*, **152** (2021), 111478. https://doi.org/10.1016/j.chaos.2021.111478

26. S. Ruan, G. S. K. Wolkowicz, Bifurcation analysis of a chemostat model with a distributed delay, *J. Math. Anal. Appl.*, **204** (1996), 786–812. https://doi.org/10.1006/jmaa.1996.0468

27. Z. Wang, B. Hu, L. Zhu, J. Lin, M. Xu, D. Wang, Hopf bifurcation analysis for Parkinson oscillation with heterogeneous delays: A theoretical derivation and simulation analysis, *Commun. Nonlinear Sci. Numer. Simul.*, **114** (2022), 106614. https://doi.org/10.1016/j.cnsns.2022.106614

28. Z. Wang, B. Hu, W. Zhou, M. Xu, D. Wang, Hopf bifurcation mechanism analysis in an improved cortex-basal ganglia network with distributed delays: An application to Parkinsons disease, *Chaos Soliton Fract.*, **166** (2023), 113022. https://doi.org/10.1016/j.chaos.2022.113022

29. T. Yu, S. Yuan, T. Zhang, The effect of delay interval on the feedback control for a turbidostat model, *J. Frankl. Inst.*, **358** (2021), 7628–7649. https://doi.org/10.1016/j.jfranklin.2021.08.003

30. X. Shi, Y. Kuang, A. Makroglou, S. Mokshagundam, J. Li, Oscillatory dynamics of an intravenous glucose tolerance test model with delay interval, *Chaos*, **27** (2017), 114324. https://doi.org/10.1063/1.5008384

AIMS Press